Arbitrary amplitude slow electron-acoustic solitons in three-electron temperature space plasmas

L. N. Mbuli, S. K. Maharaj, R. Bharuthram, S. V. Singh, and G. S. Lakhina

Citation: Physics of Plasmas **22**, 062307 (2015); doi: 10.1063/1.4922683
View online: http://dx.doi.org/10.1063/1.4922683
View Table of Contents: http://scitation.aip.org/content/aip/journal/pop/22/6?ver=pdfcov
Published by the AIP Publishing

Arbitrary amplitude slow electron-acoustic solitons in three-electron temperature space plasmas

L. N. Mbuli,[1,2] S. K. Maharaj,[1] R. Bharuthram,[2] S. V. Singh,[3] and G. S. Lakhina[3]
[1]*South African National Space Agency (SANSA) Space Science, P.O. Box 32, Hermanus 7200, Republic of South Africa*
[2]*University of the Western Cape, Robert Sobukwe Road, Bellville 7535, Republic of South Africa*
[3]*Indian Institute of Geomagnetism, New Panvel (West), Navi Mumbai 410218, India*

(Received 15 December 2014; accepted 1 June 2015; published online 24 June 2015)

We examine the characteristics of large amplitude slow electron-acoustic solitons supported in a four-component unmagnetised plasma composed of cool, warm, hot electrons, and cool ions. The inertia and pressure for all the species in this plasma system are retained by assuming that they are adiabatic fluids. Our findings reveal that both positive and negative potential slow electron-acoustic solitons are supported in the four-component plasma system. The polarity switch of the slow electron-acoustic solitons is determined by the number densities of the cool and warm electrons. Negative potential solitons, which are limited by the cool and warm electron number densities becoming unreal and the occurrence of negative potential double layers, are found for low values of the cool electron density, while the positive potential solitons occurring for large values of the cool electron density are only limited by positive potential double layers. Both the lower and upper Mach numbers for the slow electron-acoustic solitons are computed and discussed. © *2015 AIP Publishing LLC*. [http://dx.doi.org/10.1063/1.4922683]

I. INTRODUCTION

Broadband electrostatic noise (BEN) in different regions of the terrestrial magnetosphere has been associated with the linear[1,2] and nonlinear plasma waves with frequencies ranging from few Hz to above electron plasma frequencies.[3–6] The plasma instabilities, such as the electron-acoustic and ion-acoustic instabilities, have been widely studied to explain the generation of BEN in the terrestrial magnetosphere.[1,2,7] There are a number of theoretical studies that attempt to give an explanation of the generation mechanisms of BEN in the magnetosphere in terms of linear waves[8–14] and also nonlinear wave structures such as solitons and double layers.[4,5,15,16] The theory of electrostatic solitary waves, such as high-speed electron-acoustic solitons and double layers, have been proposed as a possible source of BEN with the frequency exceeding the electron plasma frequency[4,6,17–19] in space plasmas.

Both positive and negative potential solitary wave structures (propagating at the velocity ranging from about 100 to the order of about 1000 km/s[20,21]) have been observed by a number of satellites such as Viking, Polar, FAST, and S3-3 in various regions of the magnetosphere.[16,22–26] In observational studies, the bipolar (or sometimes appearing as tripolar) electric field structures with short and long periods have been interpreted in terms of electron- and ion-acoustic solitons, respectively. Recently, the FAST satellite has observed the double layer together with the ion holes (in the low potential side of the double layer) and electron holes (in the high potential side of the double layer) in auroral kilometric radiation regions.[27,28] In the plasma current sheet, the double layers were recently observed by THEMIS during the bursty bulk flow event, whereas those observed in the plasma sheet boundary layer (PSBL) were found to be associated with strong magnetic fluctuations.[26] The electrostatic double layers (accompanied by the electron holes) have also been observed by CLUSTER satellites in the separatrix region of the magnetotail.[29] Double layers are responsible for the acceleration of charged particles along the field lines resulting in mono-energetic electron and ion beam(s).[28,30] In space plasmas, the amplitude of the solitary waves usually varies from approximately 1 μV/m to 200 mV/m in the PSBL region, and is about 100 mV/m in the dayside auroral zone.[4,17,18,31]

Electrostatic high and low-speed solitons and double layers have been theoretically studied in a variety of three and four-component plasma models.[3,22,32–42] Low-speed ion-acoustic solitary waves were studied by Baboolal, Bharuthram, and Hellberg[37,43] in multi-species plasmas with two Boltzmann electron components and one or two ion components. In the investigation in Ref. 37 consisting of a positively charged ion component, they found that positive potential solitons can coexist with negative potential ion-acoustic solitons, which are limited by the occurrence of negative potential double layers. Studies on two-ion models have shown the existence of slow and fast ion-acoustic solitons.[40,44,45] Lakhina *et al.*[38] investigated existence regions of ion-acoustic and electron-acoustic solitons with arbitrary amplitudes in a three-component plasma composed of hot and cool electrons as well as ions (all treated as adiabatic). Their model showed that depending on the cool electron density, either positive or negative potential electron-acoustic solitons can occur.

A number of studies focus on the electron-acoustic solitons to understand the high-speed nonlinear electrostatic fluctuations associated with the dynamics of the electrons in

space plasma environments. Both large and small amplitude electron-acoustic solitons were studied by Mace *et al.*[46] in a plasma with Boltzmann (inertialess) hot electrons and adiabatic cool electrons as well as adiabatic ions. In this model, only negative potential electron-acoustic solitons were found to be supported. The effect of a field-aligned electron beam on the electron-acoustic solitons was theoretically studied by Berthomier *et al.*[47] in a multi-species plasma model composed of a warm electron beam, hot (Boltzmann), and cool (adiabatic) electrons, as well as cool ions (adiabatic). It was found that a warm electron beam can induce both negative and positive potential electron-acoustic solitons. In the theoretical study conducted by Cattaert, Verheest, and Hellberg,[48] it was shown that by retaining the inertia of the hot electrons in the theoretical model, the solution for both negative and positive electron-acoustic solitons can be obtained. In their study without particle beams, the inertia of the hot electrons was responsible for the positive potential solitary waves. Maharaj *et al.*[3] conducted a theoretical investigation of the existence regions of arbitrary amplitude electron-acoustic solitons for the model of Mace *et al.*[46] (where hot electrons were treated as Boltzmann) and Lakhina *et al.*[38] (where full dynamics of the species was considered). Their numerical study showed that for the model considered by Lakhina *et al.*[38] both the positive and negative potential structures were limited by either a double layer or the hot and cool electron number densities becoming complex valued for large Mach number values. However, for the model considered by Mace *et al.*[46] (where the inertia of the hot electrons was not retained) as expected from the theoretical findings of Cattaert, Verheest, and Hellberg,[48] only the negative potential electron-acoustic solitons limited by only cool electron number density were found to be supported in their model.

In this study, motivated by the linear kinetic theory study conducted by Mbuli, Maharaj, and Bharuthram,[1,2] we investigate large amplitude electron-acoustic nonlinear wave structures in a four-component plasma without any particle beams. The extension of the earlier two-electron temperature models to include a third (warm) electron population invokes the existence of both slow and fast electron-acoustic waves. We have, however, limited the scope of this study to consider only the lower phase speed (slow) electron-acoustic solitons as the higher phase speed (fast) electron-acoustic soliton results will be discussed in a forthcoming publication. We neglect the background magnetic field in our analytical and numerical analyses, which corresponds to studying the properties of nonlinear structures which propagate strictly parallel to the magnetic field.

In our study, we have treated the cold, warm, and hot electrons as adiabatic (inertial) species with polytropic index $\gamma = 3$. Most standard textbooks neglect the heat flux contribution to the energy in the calculation of the second velocity moment of the Boltzmann distribution. This is strictly justified for the case where the charged particles in a fluid have a Maxwellian distribution, as, in such a case the heat flux vanishes. We consider such a situation for the electron fluids considered here. Consequently, the fluids can be considered to be thermally insulated from each other, thus, justifying the choice of the value of $\gamma = 3$ for the polytropic indices for the cold, warm, and hot electrons for a system with one degree of freedom. Another reason for our choice of the adiabatic model for electrons is based on the observations in the Earth's plasma sheet. There are several studies concerning the thermodynamics of the plasma sheet.[52–56] All these studies show that plasma (both electrons and protons) in the plasma sheet boundary layer follow the adiabatic relationship $P_j/n_j^{\gamma} =$ constant most of time, except for a short time during substorm onsets, with adiabatic index $\gamma = 5/3$. Therefore, for the case of a one dimensional system, taking $\gamma = 3$ is justified. Furthermore, Cattaert, Verheest, and Hellberg[48] have studied the electron-acoustic soliton existence regions in a plasma consisting of ions and cool and hot electrons. They found essentially the same results for $\gamma = 3$, 2, and 1.

The layout of the paper is as follows: the theoretical model is presented in Sec. II and the numerical results and discussion are presented in Sec. III. Finally, in Sec. IV, we present a summary of our results.

II. THEORETICAL MODEL

We study large amplitude nonlinear wave structures supported in a four-component unmagnetised, homogeneous, and collisionless plasma system with cool, warm, and hot electron components, as well as cool ions, where all species are treated as adiabatic fluids. The dynamics of all species in the system are governed by the continuity, momentum, and pressure equations given by

$$\begin{aligned} &\frac{\partial n_j}{\partial t} + \frac{\partial (v_j n_j)}{\partial x} = 0, \\ &\frac{\partial v_j}{\partial t} + v_j \frac{\partial v_j}{\partial x} = -\frac{Z_j}{\mu_j}\frac{\partial \Phi}{\partial x} - \frac{1}{\mu_j n_j}\frac{\partial P_j}{\partial x}, \\ &\frac{\partial P_j}{\partial t} + v_j \frac{\partial P_j}{\partial x} + 3P_j \frac{\partial v_j}{\partial x} = 0, \end{aligned} \tag{1}$$

and Poisson's equation written as

$$\frac{\partial^2 \Phi}{\partial x^2} = -\Sigma Z_j n_j, \tag{2}$$

where n_j, v_j, P_j, and $\mu_j = m_j/m_e$, $Z_j (= -1(+1)$ for electrons(ions)), respectively, denote number density, velocity, pressure, and mass ratio of species j ($j = \mathrm{ce}, we, he, i$, representing the cool, warm, hot electrons, and the cool ions). It is important to note that in the general formalism, we treat all the species to have an equilibrium drift v_{dbjo}. However, in the numerical analysis for this particular study, we consider a totally stationary plasma with $v_{dbjo} = 0$ for all j.

All the results are presented in normalised form, with the proton-electron mass ratio taken as $m_i/m_e = 1836$, i.e., for a hydrogen plasma. The number densities are normalised by the total equilibrium plasma density $n_o = n_{io} = n_{co} + n_{ho} + n_{wo}$ and temperatures by the hot electron temperature, T_{he}. Time is normalised by the inverse total electron plasma frequency $\omega_{pe}^{-1} = (4\pi n_o e^2/\, m_e)^{-1/2}$, velocities by the hot electron thermal velocity $C_h = (T_{he}/m_e)^{1/2}$, and spatial lengths by the Debye length $\lambda_d = (T_{he}/4\pi n_o e^2)^{1/2}$.

We transform the above set of equations to a frame moving with the wave by considering $\zeta = x - Mt$, where $M(=V/C_h)$ is the normalised speed of the nonlinear wave structures. To study localised structure, such as the solitons, we assume the usual boundary conditions at equilibrium, viz., $\zeta \to \pm\infty$: $n_j \to n_{jo}$, $v_j \to v_{dbjo}$, $n_i \to 1$, $\Phi \to 0$, and $P_j \to P_{jo} \sim n_{jo}T_j$. We solve the set of Eqs. (1) for the number density of all the species in the plasma following the method by Mendoza-Briceño, Russel, and Mamun.[49]

The general expression for the number density of the plasma constituents in a four component plasma is then given by

$$n_j = \frac{n_{jo}}{\sqrt{6\delta_j}}\left[\left((M-v_{dbjo})^2 + 3\delta_j - \frac{2Z_j\Phi}{\mu_j}\right) \pm \sqrt{\left((M-v_{dbjo})^2 + 3\delta_j - \frac{2Z_j\Phi}{\mu_j}\right)^2 - 12(M-v_{dbjo})^2}\right]^{1/2}, \tag{3}$$

where $\delta_j = \frac{P_{jo}}{n_{jo}\mu_j}$. We express the above expression (Eq. (3)) in a form proposed by Ghosh, Ghosh, and Sekar-Iyengar,[50] so that n_j is written as follows:

$$n_j = \frac{n_{jo}}{2\sqrt{3\delta_j}}\left[\sqrt{\left((M-v_{dbjo}) + \sqrt{3\delta_j}\right)^2 - \frac{2Z_j\Phi}{\mu_j}} \pm \sqrt{\left((M-v_{dbjo}) - \sqrt{3\delta_j}\right)^2 - \frac{2Z_j\Phi}{\mu_j}}\right]. \tag{4}$$

It could be shown that by substituting the above expressions for n_j into Poisson's equation, (2), and integrating, leads to the energy integral-like equation given by

$$\frac{1}{2}\left(\frac{d\Phi}{d\zeta}\right)^2 + V(\Phi) = 0, \tag{5}$$

where the Sagdeev potential, $V(\Phi)$, is written as

$$V(\Phi) = \sum_j \left[\frac{n_{jo}\mu_j}{6\sqrt{3\delta_j}}\left[\left((M-v_{dbjo}) + \sqrt{3\delta_j}\right)^3 - \left(\sqrt{\left((M-v_{dbjo}) + \sqrt{3\delta_j}\right)^2 - \frac{2Z_j\Phi}{\mu_j}}\right)^3\right] \pm \frac{n_{jo}\mu_j}{6\sqrt{3\delta_j}}\left[\left((M-v_{dbjo}) - \sqrt{3\delta_j}\right)^3 - \left(\sqrt{\left((M-v_{dbjo}) - \sqrt{3\delta_j}\right)^2 - \frac{2Z_j\Phi}{\mu_j}}\right)^3\right]\right]. \tag{6}$$

In obtaining (6), we did take into account that if the species is supersonic (subsonic), the solution corresponding to the negative (positive) sign in (4) applies to ensure that the correct boundary values for the number densities are recovered at $|\xi| \to \infty$. A supersonic (subsonic) species means that the speed of the nonlinear structure is greater (smaller) than the thermal speed of that species. If we consider the phase speed of the slow EA wave, which lies between the thermal speeds of the cool and warm electrons, the ions and the cool electrons are supersonic, whereas the warm and hot electrons are subsonic. For the fast EA wave (results are not presented here), which has a phase speed which lies between the warm and hot electron thermal speeds, the only subsonic species are the hot electrons.

The second derivative of the Sagdeev potential at $\Phi = 0$ is given by

$$\frac{d^2V(\Phi)}{d\Phi^2} = \sum_j \frac{n_{jo}}{\mu_j\left((M-v_{dbjo})^2 - 3\delta_j\right)}, \tag{7}$$

and third derivative at $\Phi = 0$ is given by

$$\frac{d^3V(\Phi)}{d\Phi^3} = \sum_j \frac{3Z_j n_{jo}/\mu_j^2\left((M-v_{dbjo})^2 + \delta_j\right)}{\left((M-v_{dbjo})^2 - 3\delta_j\right)^3}. \tag{8}$$

We report here that in the limit of small amplitudes, with appropriate expansions, the Sagdeev potential, (6), reduces to

$$V(\Phi) \approx C_2\Phi^2 + C_3\Phi^3, \tag{9}$$

with the solution of (5) then yielding

$$\Phi = -\left(\frac{C_2}{C_3}\right)\mathrm{sech}^2\left(\sqrt{\left(-\frac{C_2}{4}\right)}\zeta^2\right), \tag{10}$$

with $C_2 = \frac{1}{2}\left(\frac{d^2V(\Phi)}{d\Phi^2}\right)|_{\Phi=0}$ and $C_3 = \frac{1}{6}\left(\frac{d^3V(\Phi)}{d\Phi^3}\right)|_{\Phi=0}$. It should be noted that the expression (7) set to zero provides three solutions for the critical Mach numbers. From Eqs. (9) and (10), the polarity of the solitons is determined by the sign of the third derivative (8) of the Sagdeev potential at $\Phi = 0$. For completeness of the study, the upper Mach number (M_{max}) limits beyond which soliton solutions do not exist will also be numerically computed in our study. Here, we point out the conditions that ensures the existence of the soliton solutions in our model are as follows: (i) $V(\Phi) = 0$ at $\Phi = 0$ and at $\Phi = \Phi_o$ (amplitude of a solitary wave), (ii) $\frac{dV(\Phi)}{d\Phi}|_{\Phi=0} = 0$ and $\frac{d^2V(\Phi)}{d\Phi^2}|_{\Phi=0} < 0$, (iii) positive potential solitons occur

when $V(\Phi) < 0$ for $0 < \Phi < \Phi_o (> 0)$, and (iv) negative potential solitons occur when $V(\Phi) < 0$ for $\Phi_o (< 0) < \Phi < 0$. In addition to the above soliton conditions, the double layer solution is obtained when $\frac{dV(\Phi)}{d\Phi}|_{\Phi=\Phi_o} = 0$. It is important to mention that the existence of the high-speed electron-acoustic solitons that are discussed in this manuscript are limited by either the densities of the electron species becoming unreal or the occurrence of the double layers as would be demonstrated in Sec. III. Although in our mathematical analysis presented above, we have treated all species as drifting (parallel($v_{dbjo} > 0$) or anti-parallel ($v_{dbjo} < 0$)) relative to the direction of soliton propagation, this study is restricted to the nondrifting case, viz., $v_{dbjo} = 0$ for all j.

III. NUMERICAL RESULTS AND DISCUSSIONS

We would like to point out here that solving numerically the second derivative (Eq. (7)) for roots (in this article referred to as critical Mach numbers, M_{crit}), we obtain six roots with only three positive roots having a physical meaning and the negative roots are neglected. In the lowest Mach number range, namely, $\sqrt{(3/\mu_i)T_i} < M < \sqrt{3T_{ce}}$ ion-acoustic solitons are supported. The slow electron-acoustic solitons are supported in the intermediate Mach number range ($\sqrt{3T_{ce}} < M < \sqrt{3T_{we}}$), while the fast electron-acoustic solitons occur in the highest Mach number range ($\sqrt{3T_{we}} < M < \sqrt{3}$).[17,20] Here, the main focus is on the properties and characteristics of the slow electron-acoustic solitary waves supported by our four-component plasma model. The highest-speed mode, namely, fast electron-acoustic solitary waves will be the subject of a forthcoming publication. This work is motivated by the linear theory presented by the authors, where instabilities driven by electron beam(s) such as the high-speed electron-acoustic and low-speed ion-acoustic instabilities were found to be supported.[1,2] We know from the theory of plasma waves and instabilities that such electron-acoustic and ion-acoustic instabilities may evolve into solitons in the nonlinear regime when dispersion is balanced by the nonlinearity. Although the study by Mbuli, Maharaj, and Bharuthram[1,2] was focusing on a strongly magnetised plasma and waves which propagate oblique to the magnetic field were also considered, here, we consider nonlinear structures which propagate strictly parallel to the magnetic field. We study the corresponding nonlinear waves, namely, the slow electron-acoustic solitons, which propagate at a speed greater than the linear slow electron-acoustic sound speed.

The existence domains of the electron-acoustic solitary waves is illustrated in Figure 1(a), which is demarcated into four regions, namely, regions I, II, III, and IV. In region I (where n_{co}/n_o ranges from 0.01 to 0.097), the lower curve represents the lower limits (or M_{crit} which is the phase speed of the linear wave). The increase in the M_{crit} values with cool electron concentration is consistent with an increase in the electron sound speed, $V_{se} = (n_{co}/n_o)^{1/2}(T_{\text{eff}}/m_e)^{1/2} = [n_{co}T_{we}T_{he}/m_e(n_{wo}T_{he} + n_{ho}T_{we})]^{1/2}$, where the warm electrons replace the (warm) electron beam component in the expression given in Ref. 9. Whilst the cool electrons provide the inertia for the slow EA mode, the warm and hot electrons

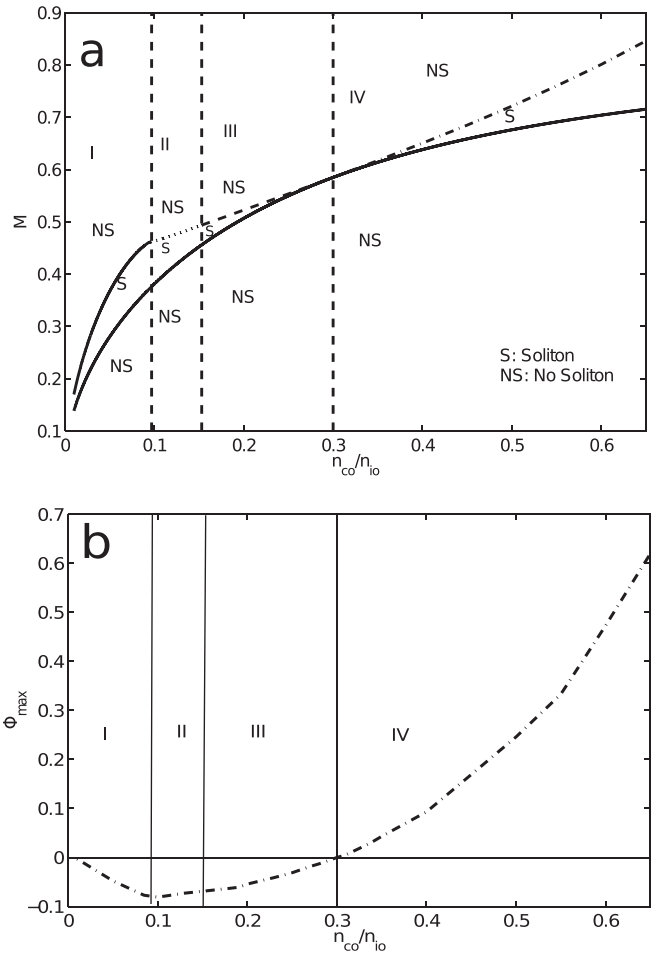

FIG. 1. Existence domains of the slow electron-acoustic solitons and double layers (a) and the maximum allowable potential (b) as a function of the cool electron number density, n_{co}/n_o. The fixed plasma parameters are $\mu_i = 1836$, $\frac{T_{ce}}{T_{he}} = 1/1000$, $\frac{T_i}{T_{he}} = 1/1000$, $\frac{T_{we}}{T_{he}} = 250/1000$, $n_{wo}/n_o = 0.3$, and $v_{dbjo} = 0$ for all species j.

contribute to an effective electron temperature, *viz.*, $T_{\text{eff}}/n_o = T_{we}T_{he}/(n_{wo}T_{he} + n_{ho}T_{we})$.

The upper curve in Figure 1 represents the upper limits (or M_{max}, which is the upper Mach number limit), which are obtained from the equation for the Sagdeev potential (6) when the cool electron number density expression (from (4) for zero particle drift, i.e., for $v_{dbjo} = 0$) given by

$$n_{ce} = \frac{n_{co}}{2\sqrt{3T_{ce}}}\left[\sqrt{\left(M + \sqrt{3T_{ce}}\right)^2 + 2\Phi} - \sqrt{\left(M - \sqrt{3T_{ce}}\right)^2 + 2\Phi}\right], \tag{11}$$

becomes complex valued, namely, whenever $(M - \sqrt{3T_{ce}})^2 + 2\Phi < 0$ or $\Phi < \Phi_{min,cool}\left(= -\frac{1}{2}\left(M - \sqrt{3T_{ce}}\right)^2\right)$. This imposes a limit on the amplitude of the solitons in this region. The value of M_{crit} is obtained by setting $C_2 = 0$ and solving this equation numerically. On the other hand, the upper Mach numbers are obtained by setting $V(\Phi = \Phi_{min,cool}) = 0$ and solving numerically to get M. Admissible soliton solutions are defined for M-values between the lower and upper curves

of Figure 1(a) in region I. The Sagdeev potential plot for $n_{co}/n_o = 0.05$ which lies in region I of Figure 1(a) is shown in Figure 2 for M ranging from $M_{crit} = 0.28016$ on the lower curve of Figure 1(a) and $M_{max} = 0.36679$ on the upper curve of Figure 1(a). The corresponding maximum electrostatic potential (beyond which (11) becomes unreal), $\Phi_{max} = -0.048$ ($n_{co}/n_o = 0.05$), for $M = M_{max}$ is shown in region I of Figure 1(b).

Soliton solutions are not found for $M > M_{max}$, e.g., in Figure 2 for $M = 0.36979$. In region II of Figure 1(a) (where n_{co}/n_o ranges from 0.097 to 0.153), we found that the upper limit to the M-values is imposed by warm electron number density, n_{we}, given by

$$n_{we} = \frac{n_{wo}}{2\sqrt{3T_{we}}}\left[\sqrt{\left(M+\sqrt{3T_{we}}\right)^2 + 2\Phi} + \sqrt{\left(M-\sqrt{3T_{we}}\right)^2 + 2\Phi}\right], \tag{12}$$

which becomes unreal (whenever $\Phi < \Phi_{min,warm}$ $(= -\frac{1}{2}(M - \sqrt{3T_{we}})^2)$) resulting in the limitation of the soliton amplitudes. In region II, the solid line represents the values of M_{crit} and the upper curve or dotted line represents the upper limits. The numerical solution for solitons in this region II is found between the solid and the dotted lines. This can be seen in Figure 3 for $n_{co}/n_o = 0.13$, where the solution for soliton exist when $M_{crit}(=0.42633) < M < M_{max}$ $(=0.47981)$. The solid line corresponds to the value $M = M_{crit}$ and the upper curve represents the upper limits. Negative potential solitons that are limited by a double layer formation is found in region III of Figure 1(a), and the corresponding amplitude of the double layers is shown in Figure 1(b) for n_{co}/n_o in a range of 0.153–0.3. In Figure 4, where $n_{co}/n_o = 0.25$, we show that as the Mach number increases the electron-acoustic soliton is limited by a double layer for $M = M_{max} = 0.55345$. We do not find a solution for solitons when $n_{co}/n_o = 0.3$ as this value represents the transition or a crossover point from the negative to positive potential solitary waves.

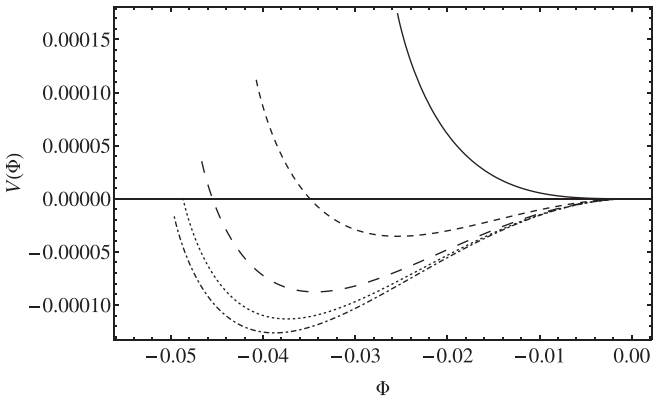

FIG. 2. The Sagdeev potential profile as a function of the electrostatic potential ϕ. The labeling parameter is the Mach number $(-)M = 0.28016$, $M = 0.34016(---)$, $M = 0.36016(- - -)$, $M = 0.36679(\cdots)$, and $M = 0.36979(- \cdot - \cdot -)$. The fixed plasma parameters are $\mu_i = 1836$, $\frac{Tce}{The} = 1/1000$, $\frac{T_i}{T_{he}} = 1/1000$, $\frac{T_{we}}{T_{he}} = 250/1000$, $n_{co}/n_o = 0.05$, $n_{wo}/n_o = 0.3$, and $v_{dbjo} = 0$ for all species j.

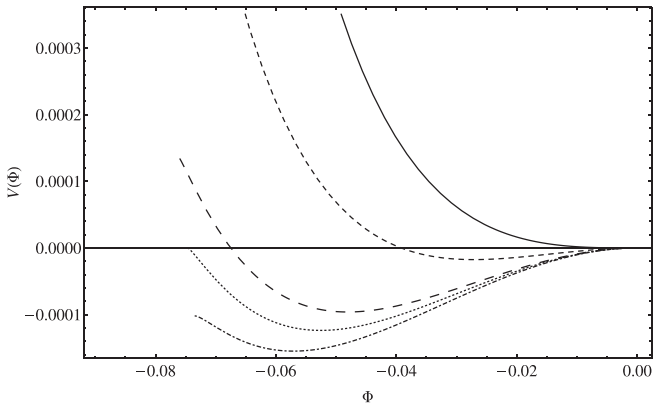

FIG. 3. The Sagdeev potential profile as a function of the electrostatic potential ϕ. The labeling parameter is the Mach number $M = 0.42633(-)$, $M = 0.45663(---)$, $M = 0.47633(- - -)$, $M = 0.47981(\cdots)$, and $M = 0.48291(- \cdot - \cdot -)$. The fixed plasma parameters are $\mu_i = 1836$, $\frac{Tce}{The} = 1/1000$, $\frac{T_i}{T_{he}} = 1/1000$, $\frac{T_{we}}{T_{he}} = 250/1000$, $n_{co}/n_o = 0.13$, $n_{wo}/n_o = 0.3$, and $v_{dbjo} = 0$ for all species j.

For $n_{co}/n_o > 0.3$, it is found that the soliton is limited by the occurrence of the positive potential double layer, whose solution is obtained for $M = M_{max}$, which lies on the upper curve of Figure 1(a) in region IV. The corresponding amplitudes of the positive potential double layers are shown in region IV of Figure 1(b). The Sagdeev potentials plot of the positive potential electron-acoustic soliton and double layer are displayed in Figure 5 for a fixed value of the cool electron density $n_{co}/n_o = 0.45$ in Figure 1(b).

Fixing the cool electron number density at $n_{co}/n_o = 0.2$, in Figure 6(a), we study the effect of the warm electron number density on the solitary waves, and show that the value of n_{wo}/n_o determines the polarity of the supported slow electron-acoustic solitons. Whereas n_{co} has the effect of increasing the electron sound speed V_{se}, and consequently, M_{crit} in Figure 1, increasing n_{wo} has the opposite effect as is apparent from Figure 6. The decrease in V_{se} (because of the reduction in the effective electron temperature) with increasing warm electron concentration explains the decrease in M_{crit} in Figure 6. As can be seen from the figure, the polarity

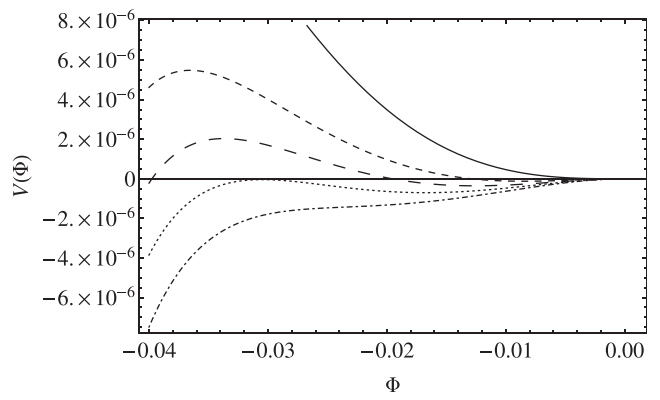

FIG. 4. The Sagdeev potential profile as a function of the electrostatic potential ϕ. The labeling parameter is the Mach number $M = 0.54985(-)$, $M = 0.55205(---)$, $M = 0.55285(- - -)$, $M = 0.55345(\cdots)$, and $M = 0.55405$ $(- \cdot - \cdot -)$. The fixed plasma parameters are $\mu_i = 1836$, $\frac{Tce}{The} = 1/1000$, $\frac{T_i}{T_{he}} = 1/1000$, $\frac{T_{we}}{T_{he}} = 250/1000$, $n_{co}/n_o = 0.25$, $n_{wo}/n_o = 0.3$, and $v_{dbjo} = 0$ for all species j.

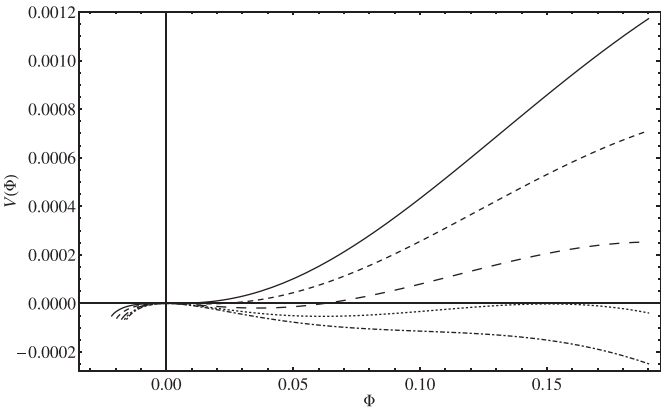

FIG. 5. The Sagdeev potential profile as a function of the electrostatic potential ϕ. The labeling parameter is the Mach number $M = 0.47731(-)$, $M = 0.48401(---), M = 0.48821(- - -), M = 0.49186(\cdots)$, and $M = 0.49435$ $(-\cdot-\cdot-)$. The fixed plasma parameters are $\mu_i = 1836$, $\frac{T_{ce}}{T_{he}} = 1/1000$, $\frac{T_i}{T_{he}} = 1/1000, \frac{T_{we}}{T_{he}} = 250/1000, n_{co}/n_o = 0.45, n_{wo}/n_o = 0.3$, and $v_{dbjo} = 0$ for all species j.

switch of the electron-acoustic soliton occurs at two points, i.e., at $n_{wo}/n_o = 0.004$ (from negative to positive) and at $n_{wo}/n_o = 0.08$ (from positive to negative). We found that in region I of Figure 6(a) for $0 < n_{wo}/n_o < 0.004$, the solutions

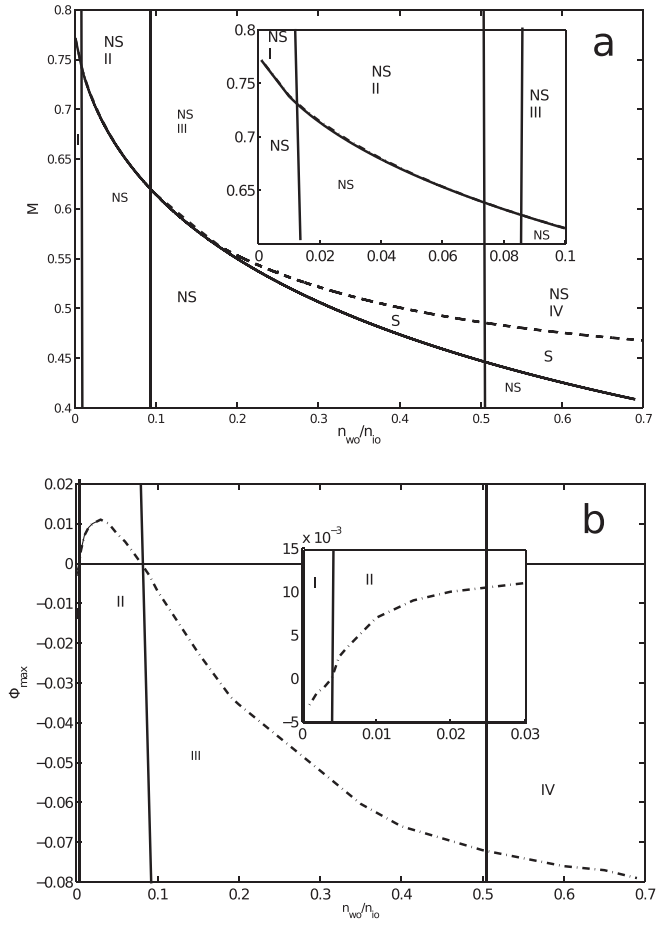

FIG. 6. Existence domains of the slow electron-acoustic solitons/double layers (a) and the maximum allowable potential (b) as a function of the warm electron number density, n_{wo}/n_o. The fixed plasma parameters are $\mu_i = 1836$, $\frac{T_i}{T_{he}} = 1/1000$, $\frac{T_{we}}{T_{he}} = 250/1000$, $n_{co}/n_o = 0.2$, and $v_{dbjo} = 0$ for all species j. The insets provide magnified views of the (a) M and (b) Φ_{max} regions for very low values of n_{wo}/n_o.

for negative potential electron-acoustic solitons as M is varied are limited by the occurrence of double layers are possible. This is not surprising as the negative potential soliton region limited by double layers was found for $n_{co}/n_o = 0.2$ in Figure 1. The transition from the negative to the positive potential solitons occurs at $n_{wo}/n_o = 0.004$. For $0.004 < n_{wo}/n_o < 0.08$, the existence of the positive potential solitons in region II of Figure 6(a) is limited by the occurrence of positive potential double layers. The maximum amplitudes of the positive potential double layers, as shown in region II of Figure 6(b), increase with increasing warm electron density, n_{wo}/n_o, and reach a maximum at $n_{wo}/n_o \sim 0.03$ (where $\Phi_{max} \sim 0.011$). Beyond $n_{wo}/n_o = 0.03$, the amplitudes of the positive potential double layers decrease with increasing n_{wo}/n_o up until the polarity switch is encountered at $n_{wo}/n_o = 0.08$. In region III of the Figure 6(a), where $0.08 < n_{wo}/n_o < 0.53$, we found that the M-values for the negative potential solitons are also limited by the occurrence of the negative potential double layers. In the range of $n_{wo}/n_o \leq 0.2$, because the upper Mach number negative double layer limits are very close to the lower limiting Mach number values (M_{crit}), this range is of little physical interest. Our results in Figure 6 are consistent with the earlier findings that the soliton regions, which lie on either side where a polarity switch occurs, are limited by double layers.[3,48] The negative potential double layer amplitudes in region III increase with increasing n_{wo}/n_o. However, in region IV (where $n_{wo}/n_o \geq 0.53$), the range of M-values for negative potential electron-acoustic solitons are found to be limited by the cool electron number density, i.e., n_{ce}, becoming complex valued. We show the maximum electrostatic potentials beyond which the cool electron number density, n_{ce}, becomes complex valued in region IV of Figure 6(b). We would like to point out that the maximum amplitudes of the negative potential slow electron-acoustic double layers in region I are very small compared to those in region III.

We now investigate the effect of varying the warm electron temperature on the existence domains of the slow electron-acoustic solitons. In Figure 7, we show the existence domains in terms of the admissible M-values. The increase in M_{crit} with T_{we} for the linear wave is expected because the effective electron temperature T_{eff} increases with increasing warm electron temperature. Having fixed $n_{wo}/n_o = 0.3$, it is expected that the first region (region I) encountered in Figure 7 (corresponding to $0 < T_{we}/T_{he} \leq 0.51$) is where negative potential solitons, which are limited by double layers occur if one refers to the previous Figure 6. In region II (where $T_{we}/T_{he} > 0.51$), negative potential solitons are supported which are limited by the warm electron density, (12), becoming complex valued. Figure 7 shows that as the parameter T_{we}/T_{he} increase both existence regions I and II which support electron-acoustic solitons broaden. The upper boundary of the range of possible M-values (dotted curve) in region I corresponds to the formation of the double layer, while in region II, it represents the warm electron number density becoming unreal.

For fixed $T_{we}/T_{he} = 0.25$, we show in Figure 8 the Sagdeev potential plot for the electron-acoustic solitons which exists for M-values greater than $M_{crit} = 0.50666$,

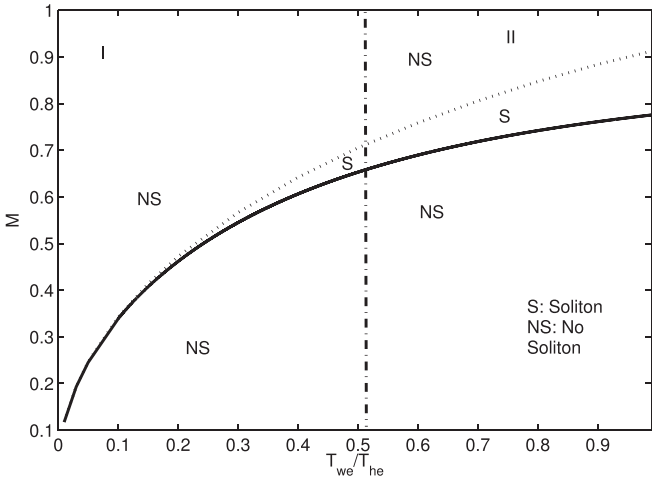

FIG. 7. Existence domains of the slow electron-acoustic solitons/double layers as a function of the warm-to-hot electron temperature, T_{we}/T_{he}. The fixed plasma parameters are $\mu_i = 1836$, $\frac{T_{ce}}{T_{he}} = 1/1000$, $\frac{T_i}{T_{he}} = 1/1000$, $n_{co}/n_o = 0.2$, $n_{wo}/n_o = 0.3$, and $v_{dbjo} = 0$ for all species j. In region I, the solitons are limited by the negative potential double layer, and in region II, the solitons are limited by the number density of the warm electrons.

where the upper boundary is due to the formation of the double layer for $M = 0.52244$. We point out here that the solitons have very small amplitudes in the narrow regions, where the upper Mach number limit (M_{max}) is almost equal to the lower Mach number limit (M_{crit}) for smaller values of the temperature of the warm electrons, and the range widens as the temperature of the warm electrons increases. For a region where the upper Mach number is much greater than the lower Mach number, the solitary wave structures have very large amplitudes. In short, we found that as the existence region of the electron-acoustic solitons widens the amplitude of the electron-acoustic structures also increases.

We would like to point out that the plasma model considered here is applicable to different regions of the terrestrial magnetosphere. The populations of the cool and warm electrons in the magnetosphere come from different regions of the ionosphere, and the hot electrons are found in the magnetosphere itself. It is due to various transport mechanisms that the ionospheric warm and cool electrons drift and enter the magnetosphere, mixing with the population of the hot electrons which are already present in the magnetosphere.[51] We have studied the properties of the high and low-speed solitons in a three electron species plasma and demonstrated that the Sagdeev pseudo-potential theory could well describe both large and small amplitude solitary structures. Coexistence of the positive and negative potential solitons in this model was not found. We do not find a region in parameter space, where the existence domains of the slow electron-acoustic type solitons is limited by the hot electron number density in all existence domains plots shown (see Figures 1(a), 1(b), 6(a), 6(b), and 7). This is not surprising since the slow EA wave phase speed lies between the cool and warm electron thermal speeds. The temperatures of the cool and warm electron species might be playing a vital role in determining which species number density becomes complex valued, and this depends on how close the speed of the nonlinear structure is to the thermal speeds which lie on either side of it.

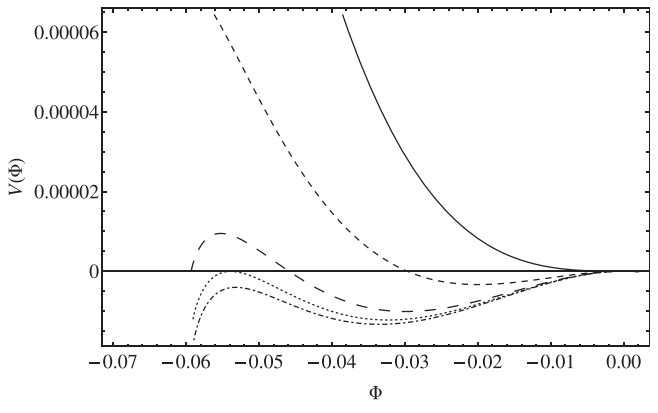

FIG. 8. The Sagdeev potential profiles as a function of the electrostatic potential for various values of Mach numbers. The parameter varying is Mach number, M, 0.50666(−), 0.51766(---), 0.52168(− − −), 0.52244(···), and 0.52278(− · − · −). The fixed plasma parameters are $\mu_i = 1836$, $\frac{T_{ce}}{T_{he}} = 1/1000$, $\frac{T_i}{T_{he}} = 1/1000$, $T_{we}/T_{he} = 250/1000$, $n_{co}/n_o = 0.2$, $n_{wo}/n_o = 0.3$, and $v_{dbjo} = 0$ for all species j.

IV. CONCLUSION

We have studied large amplitude slow electron-acoustic solitons in a four-component plasma composed of cool, warm, and hot electrons as well as ions. In our study, full dynamics of the species was considered by retaining the pressure and inertia of all the species.

The normal electrostatic modes of such a system are slow electron-acoustic and fast electron-acoustic solitons and ion-acoustic solitons. In this paper, we focus our attention on the characteristics of the slow electron-acoustic mode. We investigated the Mach number limits for the solitary waves. For slow electron-acoustic solitons, we found that both positive and negative potential solitons exist. We have found that the existence of negative and positive potential slow electron-acoustic solitons and double layers are supported. It is found that the polarity of the slow electron-acoustic solitary wave is determined by the cool and warm electron number densities. Fixing the concentration of the warm electrons, *viz.*, $n_{wo}/n_o = 0.3$, we have shown that for small concentrations of the cool electrons ($n_{co}/n_o < 0.3$), the negative potential solitons limited by the cool and warm electron number densities and negative potential double layers occur, while the positive potential electron-acoustic solitons limited by the occurrence of positive potential double layers are found to occur when $n_{co}/n_o > 0.3$. On the other hand, by fixing the cool electron density at a value of $n_{co}/n_o \sim 0.2$ and varying the warm electron number density, n_{wo}, we found that for very small values of $n_{wo}/n_o (< 0.004)$, the negative potential solitons which are limited by the occurrence of the negative potential double layers are supported in our model. For larger values of the warm electron number density, i.e., $0.004 < n_{wo}/n_o < 0.08$ positive potential solitons limited by positive potential double layers are found to exist. However, we found once again that there is an existence region, where negative potential solitons which are limited by the occurrence of the negative potential double layers are possible,

namely, for $0.08 < n_{wo}/n_o < 0.53$. For $n_{wo}/n_o \geq 0.53$, negative potential solitons are limited by the cool electron number density becoming unreal. A study of the variation of the temperature of the warm electrons, T_{we}, reveals that the Mach number range of negative potential slow electron-acoustic solitons are limited by the occurrence of double layers for $0 < T_{we}/T_{he} \leq 0.51$ and the warm electron number density becoming complex valued for $T_{we}/T_{he} > 0.51$.

ACKNOWLEDGMENTS

S.V.S. and R.B. would like to thank the Department of Science and Technology, New Delhi, India and NRF of South Africa, respectively, for the financial support. The work was done under Indo-South Africa Bilateral Project "Linear and Nonlinear studies of fluctuation phenomena in space and astrophysical plasmas." G.S.L. thanks the Indian National Science Academy, New Delhi, India for the support under the Senior Scientist Scheme.

[1]L. N. Mbuli, S. K. Maharaj, and R. Bharuthram, Phys. Plasmas **21**, 052115 (2014).
[2]L. N. Mbuli, S. K. Maharaj, and R. Bharuthram, Phys. Plasmas **20**, 122115 (2013).
[3]S. K. Maharaj, R. Bharuthram, S. V. Singh, and G. S. Lakhina, Phys. Plasmas **19**, 122301 (2012).
[4]N. Dubouloz, R. Pottelette, M. Malingre, and R. A. Treumann, Geophys. Res. Lett. **18**, 155, doi:10.1029/90GL02677 (1991).
[5]N. Dubouloz, R. A. Treumann, R. Pottelette, and M. Malingre, J. Geophys. Res. **98**, 17415, doi:10.1029/93JA01611 (1993).
[6]C. L. Grabbe, Geophys. Res. Lett. **29**, 072122, doi:10.1029/2002GL015265 (2002).
[7]E. J. Koen, A. Collier, and S. K. Maharaj, Phys. Plasmas **21**, 072122 (2014).
[8]S. V. Singh and G. S. Lakhina, Planet. Space Sci. **49**, 107 (2001).
[9]A. Sooklal and R. L. Mace, Phys. Plasmas **11**, 1996 (2004).
[10]R. L. Mace and M. A. Hellberg, J. Geophys. Res. **98**, 5881, doi:10.1029/92JA02900 (1993).
[11]T. K. Baluku, M. A. Hellberg, and R. L. Mace, J. Geophys. Res. **116**, A04227, doi:10.1029/2010JA016112 (2011).
[12]S. V. Singh, M. A. Reddy, and G. S. Lakhina, Adv. Space Res. **43**, 1940 (2009).
[13]D. Schriver and M. Ashour-Abdalla, J. Geophys. Res. **92**, 5807, doi:10.1029/JA092iA06p05807 (1987).
[14]C. Grabbe, J. Geophys. Res. **94**, 17299, doi:10.1029/JA094iA12p17299 (1989).
[15]A. Kakad, S. V. Singh, R. V. Reddy, G. S. Lakhina, and S. G. Tagare, Adv. Space Res. **43**, 1945 (2009).
[16]M. Malingre, R. Pottelette, R. A. Treumann, and M. Berthomier, J. Geophys. Res. **102**, 19861, doi:10.1029/97JA01375 (1997).
[17]G. S. Lakhina, S. V. Singh, A. P. Kakad, and J. S. Pickett, J. Geophys. Res. **116**, A10218, doi:10.1029/2011JA016700 (2011).
[18]S. V. Singh, G. S. Lakhina, R. Bharuthram, and S. R. Pillay, Phys. Plasmas **18**, 083705 (2011).
[19]A. Teste and G. K. Parks, Phys. Rev. Lett. **102**, 075003 (2009).
[20]G. S. Lakhina, S. V. Singh, and A. P. Kakad, Adv. Space Res. **47**, 1558 (2011).
[21]R. Pottelette and M. Berthomier, Nonlinear Processes Geophys. **16**, 373 (2009).
[22]M. Temerin, K. Cerny, W. Lotko, and F. S. Mozer, Phys. Rev. Lett. **48**, 1175 (1982).
[23]R. Bostrom, G. Gustafsson, B. Holback, G. Holmgreen, H. Koskinen, and P. Kintner, Phys. Rev. Lett. **61**, 82 (1988).
[24]H. E. J. Koskinen, R. Lundin, and B. Holback, J. Geophys. Res. **95**, 5921, doi:10.1029/JA095iA05p05921 (1990).
[25]P. O. Dovner, A. I. Erikkson, R. Bostrom, and B. Holback, Geophys. Res. Lett. **21**, 1827, doi:10.1029/94GL00886 (1994).
[26]R. E. Ergun, L. Andersson, J. Tao, V. Angelopoulos, J. Bonnell, J. P. McFadden, D. E. Larson, S. Eriksson, T. Johansson, C. M. Cully, D. N. Newman, M. V. Goldman, A. Roux, O. LeContel, K. H. Glassmeier, and W. Baumjohann, Phys. Rev. Lett. **102**, 155002 (2009).
[27]M. Berthomier, R. Pottelette, M. Malingre, and Y. Khotyaintsev, Phys. Plasmas **7**, 2987 (2000).
[28]R. Pottelette, R. A. Truemann, and E. Georgescu, Nonlinear Processes Geophys. **11**, 197 (2004).
[29]R. Wang, Q. Lu, Y. V. Khotyaintsev, M. Volwerk, A. Du, R. Nakumara, W. D. Gonzalez, X. Sun, W. Baumjohann, T. Li, T. Zhang, A. N. Fazakerley, C. Huang, and M. Wu, Geophys. Res. Lett. **41**, 4851, doi:10.1002/2014GL061157 (2014).
[30]R. Pottelette, M. Berthomier, and J. Pickett, Ann. Geophys. **32**, 677 (2014).
[31]R. E. Ergun, L. Andersson, C. W. Carlson, D. N. Newman, and M. V. Goldman, Nonlinear Processes Geophys. **10**, 45 (2003).
[32]M. A. Hellberg and F. Verheest, J. Plasma Phys. **76**, 277 (2010).
[33]T. M. Baluku and M. A. Hellberg, Phys. Plasmas **19**, 012106 (2012).
[34]T. M. Baluku, M. A. Hellberg, and F. Verheest, Europhys. Lett. **91**, 15001 (2010).
[35]S. N. Saini, I. Kourakis, and M. A. Hellberg, Phys. Plasmas **16**, 062903 (2009).
[36]R. Bharuthram and P. K. Shukla, Phys. Fluids **29**, 3214 (1986).
[37]S. Baboolal, R. Bharuthram, and M. A. Hellberg, J. Plasma Phys. **44**, 1 (1990).
[38]G. S. Lakhina, A. P. Kakad, S. V. Singh, and F. Verheest, Phys. Plasmas **15**, 062903 (2008).
[39]M. A. Hellberg and F. Verheest, Phys. Plasmas **15**, 062307 (2008).
[40]G. S. Lakhina, S. V. Singh, and A. P. Kakad, Phys. Plasmas **21**, 062311 (2014).
[41]B. Kakad, A. P. Kakad, and Y. Omura, J. Geophys. Res. **119**, 5589, doi:10.1002/2014JA019798 (2014).
[42]S. V. Singh and G. S. Lakhina, Commun. Nonlinear Sci. Numer. Simul. **23**, 274 (2015).
[43]S. Baboolal, R. Bharuthram, and M. A. Hellberg, J. Plasma Phys. **40**, 163 (1988).
[44]F. Nsengiyumva, M. A. Hellberg, F. Verheest, and R. L. Mace, Phys. Plasmas **21**, 102301 (2014).
[45]G. S. Lakhina, S. V. Singh, A. P. Kakad, F. Verheest, and R. Bharuthram, Nonlinear Processes Geophys. **15**, 903 (2008).
[46]R. L. Mace, S. Baboolal, R. Bharuthram, and M. A. Hellberg, J. Plasma Phys. **45**, 323 (1991).
[47]M. Berthomier, R. Pottelette, M. Malingre, and Y. Khotyaintsev, Phys. Plasmas **7**, 2987 (2000).
[48]T. Cattaert, F. Verheest, and M. A. Hellberg, Phys. Plasmas **12**, 042901 (2005).
[49]C. A. Mendoza-Briceño, S. M. Russel, and A. A. Mamun, Planet. Space Sci. **48**, 599 (2000).
[50]S. S. Ghosh, K. K. Ghosh, and A. N. Sekar-Iyengar, Phys. Plasmas **3**, 3939 (1996).
[51]R. Pottelette, R. E. Ergun, R. A. Treumann, M. Berthomier, C. W. Carlson, J. P. McFadden, and I. Roth, Geophys. Res. Lett. **26**, 2629, doi:10.1029/1999GL900462 (1999).
[52]C. K. Goertz and W. Baumjohann, J. Geophys. Res. **96**, 20991, doi:10.1029/91JA02128 (1991).
[53]C. Y. Huang, L. A. Frank, G. Rostoker, J. Fennell, and D. G. Mitchell, J. Geophys. Res. **97**, 1481, doi:10.1029/91JA02517 (1992).
[54]R. L. Kaufmann and W. R. Patterson, J. Geophys. Res. **114**, A00D04, doi:10.1029/2008JA014030 (2009).
[55]C. P. Wang, L. R. Lyons, R. A. Wolf, T. Nagai, J. M. Weygang, and A. T. Y. Lui, J. Geophys. Res. **114**, A00D02, doi:10.1029/2008JA013849 (2009).
[56]X. Y. Zhou, C. T. Russell, and D. G. Mitchell, J. Geophys. Res. **102**, 14425, doi:10.1029/97JA00683 (1997).